# Eight Amino Acids Form the ATP Recognition Site of $Na^+/K^+$-ATPase†

Martin Kubala,[‡,§] Jan Teisinger,[‡] Rüdiger Ettrich,[‡,||] Kateřina Hofbauerová,[‡,⊥] Vladimír Kopecký, Jr.,[‡,§,⊥] Vladimír Baumruk,[§] Rita Krumscheid,[@] Jaromír Plášek,[§] Wilhelm Schoner,[@] and Evžen Amler*[,‡]

*Institute of Physiology, Academy of Sciences of the Czech Republic, Vídeňská 1083, 14220 Prague, Czech Republic, Laboratory of High Performance Computing, Institute of Physical Biology USB and Institute of Landscape Ecology ASCR, Zámek 136, 37333 Nové Hrady, Czech Republic, Department of Biochemistry, Faculty of Science, Charles University, Albertov 2030, 12840 Prague, Czech Republic, Institute of Physics, Charles University of Prague, Ke Karlovu 5, 12116 Prague, Czech Republic, and Institute of Biochemistry and Endocrinology, Justus-Liebig-University Giessen, Frankfurter Strasse 100, D-35392 Giessen, Germany*

*Received January 29, 2003; Revised Manuscript Received April 11, 2003*

ABSTRACT: Point mutations of a part of the $H_4-H_5$ loop ($Leu^{354}-Ile^{604}$) of $Na^+/K^+$-ATPase have been used to study the ATP and TNP-ATP binding affinities. Besides the previously reported amino acid residues $Lys^{480}$, $Lys^{501}$, $Gly^{502}$, and $Cys^{549}$, we have found four more amino acid residues, viz., $Glu^{446}$, $Phe^{475}$, $Gln^{482}$, and $Phe^{548}$, completing the ATP-binding pocket of $Na^+/K^+$-ATPase. Moreover, mutation of $Arg^{423}$ has also resulted in a large decrease in the extent of ATP binding. This residue, localized outside the binding pocket, seems to play a key role in supporting the proper structure and shape of the binding site, probably due to formation of a hydrogen bond with $Glu^{472}$. On the other hand, only some minor effects were caused by mutations of $Ile^{417}$, $Asn^{422}$, $Ser^{445}$, and $Glu^{505}$.

The $Na^+/K^+$-ATPase (EC 3.6.3.9, sodium pump) is an enzyme transporting sodium and potassium ions across the plasmatic membrane. The enzyme of the $P_2$ subtype of the P-type ATPase superfamily is a heterodimer of a 100 kDa catalytic subunit with 10 transmembrane segments and a heavily glycosylated $\beta$-subunit of ~55 kDa (*1*). Two ATP-binding sites have been detected on the $Na^+/K^+$-ATPase, the high- and low-affinity ATP sites with approximate $K_d$ values of 1 $\mu$M ($E_1$-ATP site) and 200 $\mu$M ($E_2$-ATP site), respectively (*2*).

When the three-dimensional structure (0.26 nm resolution) of the $Ca^{2+}$-ATPase pump of sarcoplasmic reticulum became known (*3*, *4*), the possibility of deducing by restraint-based comparative modeling the analogous three-dimensional structure of the $H_4-H_5$ loop of $Na^+/K^+$-ATPase arose (*5*). *In silico* docking of ATP to the loop revealed in analogy to the $Ca^{2+}$-ATPase the existence of a single ATP-binding site in the N-domain only (*5*). Three large domains have been identified, designated as N (nucleotide), P (phosphorylation), and A (actuator), on the cytosolic site. Domains N and P reside on the loop between transmembrane helices 4 and 5 ($H_4-H_5$ loop), while the A-domain is formed by the $H_2-H_3$ loop. Notably, the isolated $H_4-H_5$ loop expressed in *Escherichia coli* has been shown to retain properties of the whole enzyme, such as TNP-ATP binding (*6*−*9*) and phosphatase activity (*8*). This is in accordance with recent findings estimated from the crystals of $Na^+/K^+$-ATPase at 0.9 nm resolution (*10*). The recently published crystal structure of $Ca^{2+}$-ATPase in the $E_2$ conformation revealed large translation and rotation motions of the cytoplasmic domains and transmembrane segments (*4*). Despite these enormous conformational changes, mutual positions of amino acid residues within each domain seem to exhibit only very small changes, except for the couple of "hinge" residues and those at the A−P interface (*4*).

On the basis of the restraint-based comparative modeling, we recently calculated the three-dimensional structure of the large cytoplasmic loop of the $Na^+/K^+$-ATPase (*5*). The model clearly shows that the $H_4-H_5$ loop contains only one ATP-binding site; recently published results support this suggestion (*11*−*13*). The ATP-binding site has been localized on the N-domain ($Arg^{378}-Arg^{589}$), which is clearly separated from the P-domain ($Leu^{354}-Asn^{377}$ and $Ala^{590}-Leu^{773}$) where the phosphorylation site ($Asp^{369}$) is located (*5*).

Many experiments were performed in an effort to better understand the interaction of ATP with the enzyme. Chemical modification of $Lys^{480}$ (*14*−*16*), $Lys^{501}$ (*17*−*19*), $Gly^{502}$ (*16*), and $Cys^{549}$ (*36*) strongly inhibited ATP binding, suggesting that these residues are a part of an ATP-binding pocket. Furthermore, site-directed mutagenesis of $Glu^{472}$ and $Lys^{480}$ led to substantial restriction of ATP binding (*20*). It was shown that single mutations of $Phe^{475}$, $Lys^{480}$, $Lys^{501}$, and $Arg^{544}$ led to a substantial suppression of activity of the enzyme (*12*). An NMR study of the $Ca^{2+}$-ATPase showed that residues $Thr^{441}$, $Phe^{487}$, $Lys^{492}$, and $Lys^{515}$ are localized in the proximity of the bound ATP molecule. In addition, approximately 20 other amino acids in the $Met^{361}-Val^{363}$,

† This work was supported by Grants GACR 204/01/0254, 204/01/1001, and 309/02/1479 and MSMT 123100001, 113100001, 113200001 and Research Projects AVOZ 5011922 and CZE00/033.

* To whom correspondence should be addressed: Institute of Physiology, Academy of Sciences of the Czech Republic, Vídeňská 1083, 142 20 Prague, Czech Republic. Phone: +420 241062792. Fax: +420 241062249. E-mail: amler@biomed.cas.cz.

‡ Academy of Sciences of the Czech Republic.

§ Charles University of Prague.

|| Institute of Physical Biology USB and Institute of Landscape Ecology ASCR.

⊥ Charles University.

@ Justus-Liebig-University Giessen.

10.1021/bi034162u CCC: $25.00 
Published on Web 05/09/2003

Leu$^{419}$−Ser$^{424}$, Glu$^{439}$−Glu$^{442}$, Met$^{494}$−Ser$^{503}$, Val$^{514}$−Ile$^{522}$, and Cys$^{561}$−Thr$^{569}$ regions were proposed to be less important participants in ATP binding (*21*).

Comparison with the sequence of the $Na^+/K^+$-ATPase led to the suggestion that the corresponding residues, viz., Ser$^{445}$, Phe$^{475}$, Lys$^{480}$, and Lys$^{501}$, and in addition Glu$^{446}$ are part of the ATP-binding site (*22*). Our preliminary report proved (*9*) that mutation of Glu$^{446}$ and Phe$^{475}$ led to strong inhibition of ATP binding. Mutation of Ser$^{445}$, however, had no effect.

According to the predictions of our model, Gln$^{482}$, Glu$^{505}$, Phe$^{548}$, and Cys$^{549}$ also contribute to the formation of a positively charged ATP-binding pocket. To verify these suggestions and to test possible discrepancies, site-directed mutagenesis of Ile$^{417}$, Asn$^{422}$, Arg$^{423}$, Phe$^{475}$, Glu$^{505}$, and Phe$^{548}$ was performed. A fluorescent analogue of ATP, TNP-ATP, was used to test the effect of these mutations on the binding of both TNP-ATP and ATP.

## MATERIALS AND METHODS

Chemicals were obtained from Sigma-Aldrich. TNP-ATP was from Molecular Probes (Eugene, OR). Pfu-Polymerase was from Stratagene (La Jolla, CA). Restriction endonucleases *Bam*HI and *Eco*RI were from Promega (Mannheim, Germany). The pGEX-2T expression vector was from Amersham Biosciences (Freiburg, Germany). *E. coli* XL1 blue cells were from Stratagene. BL21DE3 cells were a generous gift from J. Naprstek (Charles University). DNA sequencing was performed on an ABI Prism automated sequencer at the facility of the Academy of Sciences of the Czech Republic. DNA sequencing was carried out with an automated sequencer (ABI Prism).

*Construction of the Protein Expression Vector pGEX-$H_4$−$H_5$.* The $H_4$−$H_5$ loop sequence (WT) was prepared from the sequence of the α-subunit of mouse brain $Na^+/K^+$-ATPase by polymerase chain reaction. Construction of the expression plasmid pGEX-2T containing the cDNA for the $H_4$−$H_5$ loop (Leu$^{354}$−Ile$^{604}$) was described previously (*23*). Site-directed mutagenesis was carried out using polymerase chain reaction with the QuickChange kit (Stratagene) according to the manufacturer's protocol. Sequences of sense primers used for site-directed mutagenesis were as follows: I417NN422A, 5′-C AGA AAT GCT GGT CTC TGT GCC AGG GCA GTG TTT CAG GCT AAC C-3′; R423L, 5′-GA ATT GCT GGT CTC TGT AAC CTG GCA GTG TTT CAG GCT AAC C-3′; Q482L, 5′-C TCC ACC AAC AAG TAC CTG CTC TCC ATT CAC AAG AAC CC-3′; E505Q, 5′-GTG ATG AAG GGC GCC CCA CAA AGG ATC CTG GAC CGA TGC-3′; F548G, 5′-GGA GAG CGT GTG CTA GGT GGC TGC CAC CTC CTT CTG CCT GAC-3′; and F548Y, 5′-GGA GAG CGT GTG CTA GGT TAC TGC CAC CTC CTT CTG CCT GAC G-3′. The altered nucleotides are underlined.

*Expression and Purification of the $H_4$−$H_5$ Loop.* Proteins were expressed in *E. coli* BL21 cells grown in fresh LB medium at 37 °C. The purification of our GST fusion proteins using a Sephadex 4B column was described in detail previously (*9*). The purity of proteins was checked by 12% (w/v) SDS−PAGE, and their concentration was estimated by using the Bradford method (*24*). Purified proteins were stored in 50 mM Tris-HCl at pH 7.5 and −20 °C.

*Molecular Modeling.* Molecular modeling of the $H_4$−$H_5$ cytoplasmic loop of the α-subunit of $Na^+/K^+$-ATPase ranging from L354 to L773 has been reported earlier (*5*). A model of the cytopasmic loop of mouse brain $Na^+/K^+$-ATPase from Leu$^{354}$ to Ile$^{604}$ was generated by analogy to $Ca^{2+}$-ATPase with the MODELLER6 package. (*25*). The alignment published for the pig kidney sequence (*5*) was used, and the respective residues were changed to the mouse brain ones. For model refinement and minimization, the SYBYL package with the TRIPOS force field (TRIPOS Associates Inc.) was used. The tertiary structure models were checked with ProCheck (*26*), showing *g* factors in the same range as reported in ref *5* for the pig kidney loop. Docking of ATP was explored with AutoDock (*27*). With the complete modeling, energy minimization, and docking procedure, we used exactly the parameters and methods published for pig kidney $Na^+/K^+$-ATPase (*14*). Computational site-directed mutagenesis was performed on our recently published model structure (*5*) using the program TRITON (*28*).

*FTIR Spectroscopy.* Infrared spectra were recorded at room temperature with the Bruker IFS-66/S FT-IR spectrometer using a standard source, a KBr beam splitter, and an MCT detector. Usually 4000 scans were collected with 4 $cm^{-1}$ spectral resolution and a Happ-Genzel apodization function. Samples were placed in a demountable cell (Graseby Specac) consisting of a pair of $CaF_2$ windows and a 12 μm Mylar spacer. The spectral contribution of a buffer in the carbonyl stretching region was carefully corrected following the standard algorithm (*29*).

*TNP-ATP Binding to the Recombinant $H_4$−$H_5$ Loop.* The emission intensity of the fluorescence probe TNP-ATP [2′,3′-*O*-(2,4,6-trinitrophenyl)adenosine 5′-triphosphate, trisodium salt; from Molecular Probes] is sensitive to the polarity of its environment (*30*). To perform probe binding assays with recombinant GST-bound $H_4$−$H_5$ loops, aliquots of TNP-ATP were subsequently added to pure buffer and then to the protein solutions. The binding of the fluorescent probe to the investigated proteins was revealed by the increase in probe fluorescence intensity (*9*, *31*). There was no GST interference observed in our experiments. For the details of our experimental setup, see ref *9*.

*TNP-ATP Binding to Fusion Proteins: Titration Assays and Assessment of Dissociation Constants.* Signals of buffer and protein (if present) were collected before addition of TNP-ATP, and this value was subtracted from all further raw data as a background. Correction for volume dilution of both protein and probe concentrations was done. Then the corrected fluorescence intensity was normalized using the fluorescence intensity from a 1 μM TNP-ATP solution in a pure buffer as a unit. The dependence of this normalized fluorescence intensity on the total concentration of TNP-ATP in the sample was then fitted to the following equation (for derivation of this equation, see ref *32*)

$$F = [\mathrm{P}] + {}^1\!/_2(\gamma - 1)\left[[\mathrm{P}] + [\mathrm{E}] + K_\mathrm{D} - \sqrt{([\mathrm{P}] + [\mathrm{E}] + K_\mathrm{D})^2 - 4[\mathrm{P}][\mathrm{E}]}\right]$$

where $F$ is the normalized fluorescence intensity, [P] the concentration of TNP-ATP, [E] the concentration of the enzyme, $\gamma$ the enhancement in relative fluorescence intensity upon binding of a free probe molecule to the investigated protein, and $K_\mathrm{D}$ the dissociation constant. The fluorescence enhancement factor $\gamma$ for TNP-ATP binding to fusion

proteins was determined to be 7 ± 0.7. All parameters except $K_D$ were kept constant during the fitting procedure. All values are presented as means ± SEM (standard error of the mean) from at least three independent measurements.

*Assessment of Binding of ATP to Fusion Proteins*. GST fusion proteins were incubated with TNP-ATP in the presence of ATP at pH 7.5. Competition between the fluorescence probe and ATP resulted in a lower rate of binding of TNP-ATP to protein (i.e., lower fluorescence intensity) compared to that from experiments where no ATP was present. The experimental procedure was the same as that for the assessment of TNP-ATP binding to proteins, except that measurements were performed in 50 mM Tris-HCl and 20 mM ATP at pH 7.5 (buffer pH adjusted to 7.5 after addition of ATP). The ATP was diluted upon addition of protein, so the initial concentration of ATP ranged from 19.3 to 19.8 mM for all mutants, except F548Y (9.2 mM).

*Calculation of the Dissociation Constant for Binding of ATP to Fusion Proteins.* The signal of buffer, ATP, and protein was collected before addition of TNP-ATP, and this value was subtracted from all further raw data as a background. Corrections for volume dilution of ATP, protein, and probe concentrations were done. The fluorescence intensity was normalized as described above. The dependence of fluorescence intensity on the concentration of TNP-ATP was fitted to the following equation, in good approximation describing the model where the fluorescence probe and ATP compete for the same binding site

$$F = [\mathrm{P}] + {}^1\!/_2(\gamma - 1)\left[[\mathrm{P}] + [\mathrm{E}] + K_\mathrm{P} + [\mathrm{A}]\frac{K_\mathrm{P}}{K_\mathrm{A}} - \sqrt{\left([\mathrm{P}] + [\mathrm{E}] + K_\mathrm{P} + [\mathrm{A}]\frac{K_\mathrm{P}}{K_\mathrm{A}}\right)^2 - 4[\mathrm{P}][\mathrm{E}]}\right]$$

where [A] represents the concentration of ATP, $K_P$ the dissociation constant of TNP-ATP, and $K_A$ the dissociation constant of ATP (*33*). All parameters except $K_A$ were kept constant during the fitting procedure, and the dissociation constant of TNP-ATP was estimated as described above. All values are presented as means ± SEM from at least three independent measurements.

## RESULTS

*Point Mutations Did Not Cause a Change in the Secondary Structure of the $H_4$−$H_5$ Loop in Molecular Modeling. (1) Molecular Modeling.* The point mutations have been selected, on the basis of the molecular model (*5*) constructed in analogy to the sarcoplasmic reticulum $Ca^{2+}$-ATPase (*3*). We have docked into our $H_4$−$H_5$ loop the molecule of ATP. Such modeling suggested that, in addition to the other amino acid residues reported previously, three more amino acid residues, viz., Q482, F548, and E505, participate in the recognition of TNP-ATP and/or ATP. In contrast, a stretch of amino acids between $Ile^{417}$ and $Val^{425}$ lies outside the binding pocket. Thus, we used point mutations to test this interaction. The following mutations have been employed: I417NN422A, R423L, Q482L, E505Q, F548G, and F548Y. Phenylalanine 548 was replaced not only with tyrosine but also with glycine to exclude the possibility that a bulky tyrosine might cause sterical hindrance to ATP binding which should not happen with the much smaller glycine. Our model was also applied to predict the effect of all the point mutations on the secondary structure of the $H_4$−$H_5$ loop. The three-dimensional structure was predicted for all mutations (i.e., I417NN422A, R423L, Q482L, E505Q, F548G, and F548Y). Molecular modeling did not predict any change in the folding structure of the nucleotide binding domain (N-domain) caused by any of the point mutations that were used.

Table 1: Secondary Structure of the $H_4$−$H_5$ Loop Protein with Point Mutations Predicted by Computer Modeling and Determined by FTIR Spectroscopy[a]

| sample | α-helix | β-sheet | β-turn | bend | other |
|---|---|---|---|---|---|
| R423L | 20.6 | 25.5 | 14.6 | 11.3 | 28.0 |
| Q482L | 23.7 | 22.4 | 14.7 | 10.3 | 28.8 |
| E505Q | 23.0 | 23.7 | 14.8 | 9.9 | 28.7 |
| F548G | 21.5 | 25.0 | 14.8 | 10.5 | 28.3 |

[a] The influence of the point mutation on the secondary structure was estimated from the infrared spectra of GST fusion proteins by the least-squares analysis of the amide I and amide II bands using the reference set (*29*).

Table 2: Dissociation Constants of TNP-ATP and ATP Binding to the Proteins with Point Mutations[a]

| protein | *n* | $K_D$(TNP-ATP) (μM) | Δ*G*(TNP-ATP) (kJ/mol) | *n* | $K_D$(ATP) (mM) | Δ*G*(ATP) (kJ/mol) |
|---|---|---|---|---|---|---|
| I417NN422A | 3 | 9.4 ± 0.4 | 2.7 | 4 | 8 ± 2 | 0.6 |
| R423L | 6 | 18 ± 2 | 4.3 | 4 | 31 ± 9 | 4.0 |
| Q482L | 5 | 22 ± 2 | 4.8 | 5 | 16 ± 4 | 2.3 |
| E505Q | 5 | 7.0 ± 0.4 | 2.0 | 4 | 6.2 ± 0.6 | 0 |
| F548G | 5 | 21 ± 4 | 4.7 | 5 | 11 ± 3 | 1.4 |
| F548Y | 3 | 26 ± 2 | 5.2 | 3 | 24 ± 18 | 3.3 |

[a] Dissociation constants for binding of TNP-ATP and ATP to GST fusion proteins containing point mutations were calculated as described in Materials and Methods. Data are presented as means ± the standard error of the mean from *n* independent measurements. Dissociation constants for WT have already been determined: 3.1 μM for TNP-ATP binding and 6.2 mM for ATP binding.

*(2) Infrared Spectroscopy.* To test our conclusion obtained from molecular modeling, Fourier transform infrared spectroscopy was used to examine the secondary structure of mutants F548G, F548Y, E505Q, Q482L, and R423L. No secondary structure of any of the mutants that were tested was significantly changed, suggesting no influence of the point mutations on the loop structure (Table 1). The spectra that were obtained were evaluated by the least-squares analysis (LSA) of the amide I and amide II bands. The estimated secondary structure was very similar for all samples. Subsequently, the secondary structure determined by molecular modeling has been confirmed also experimentally, and we can conclude that none of the point mutations used in our experiments influenced the secondary structure of the $H_4$−$H_5$ loop.

*The Dissociation Constants for TNP-ATP Binding Were Significantly Increased for All Our Point Mutations.* The extent of TNP-ATP binding to all six mutants, viz., I417NN422A, R423L, Q482L, E505Q, F548G, and F548Y, was measured as the increase in fluorescence when the $H_4$−$H_5$ loop−GST fusion protein was titrated with TNP-ATP (Figure 1). There was no fluorescence enhancement and, consequently, no TNP-ATP binding observed in the presence of the GST protein alone. However, the presence of the $H_4$−

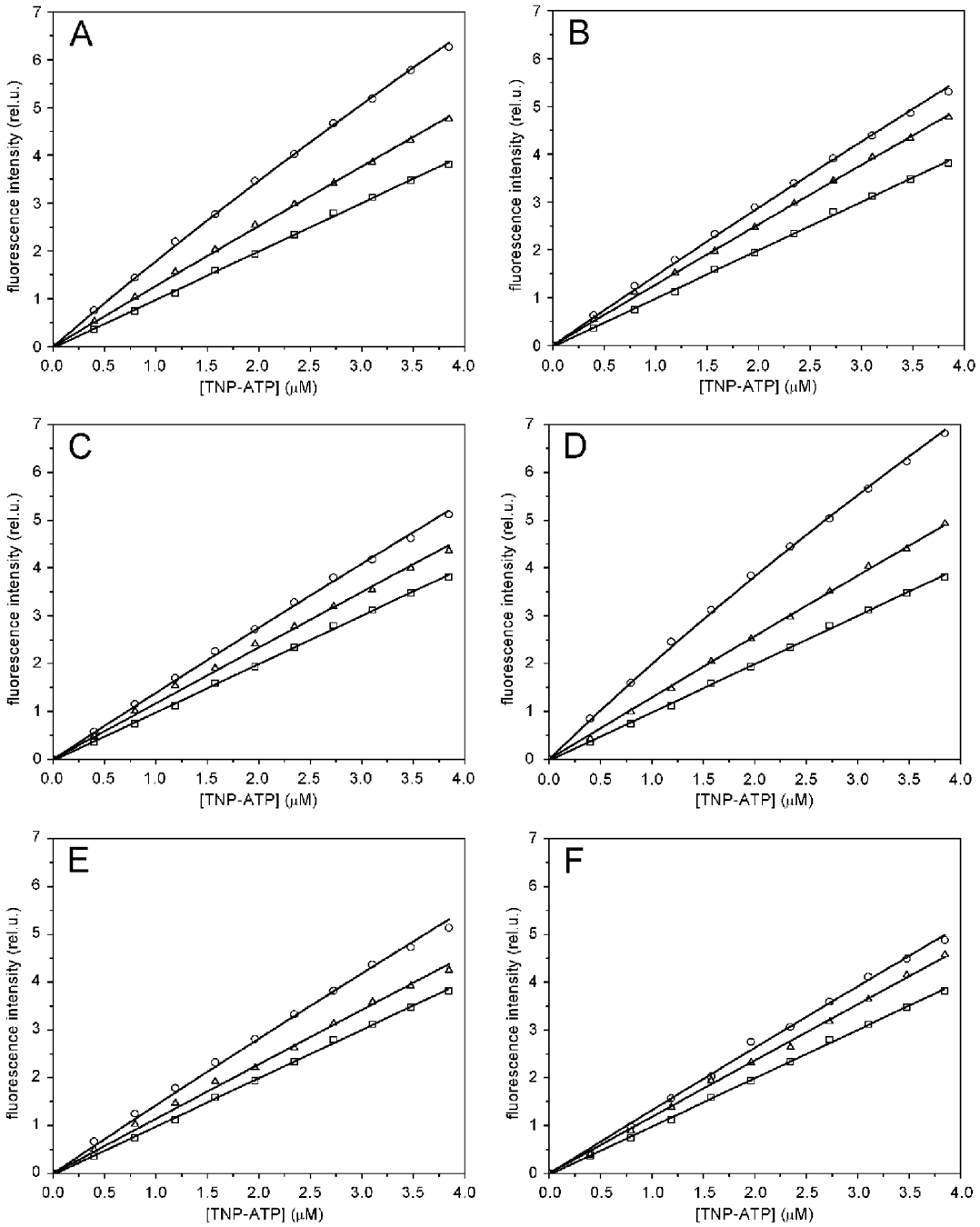


FIGURE 1: TNP-ATP binding to the $H_4-H_5$ loop protein with point mutations in the presence and absence of ATP. GST fusion proteins (1.6 $\mu$M) containing point mutations [(A) I417NN422A, (B) R423L, (C) Q482L, (D) E505Q, (E) F548G, and (F) F548Y] were titrated with increasing amounts of TNP-ATP in 50 mM Tris-HCl at pH 7.5 (○). Binding of TNP-ATP resulted in an increase in the fluorescence intensity. Similar experiments were then performed in 50 mM Tris-HCl and 20 mM ATP at pH 7.5 (△); the pH of the buffer was adjusted to 7.5 after addition of ATP. Some of the binding sites were occupied by ATP, resulting in a lower initial slope of fluorescence intensity. For comparison, titration in pure buffer in the absence of any protein is shown (□). Note that the same result was obtained, when only the GST protein itself or ATP was present (data not shown).

$H_5$−GST fusion protein resulted in an increase in steady-state fluorescence, indicating TNP-ATP binding to the $H_4-H_5$ loop. Analysis of the increase in TNP-ATP fluorescence as a function of the fluorophore concentration by a Scatchard plot revealed clearly in all tested mutants a single binding site for TNP-ATP alone. We found that the dissociation constant ($K_D$) for TNP-ATP increased from a value of 3.1 ± 0.2 $\mu$M for the WT protein (*9*) to 9.4 ± 0.4 $\mu$M for I417NN422A, 18 ± 2 $\mu$M for R423L, 22 ± 2 $\mu$M for Q482L, 7.0 ± 0.4 $\mu$M for E505Q, 21 ± 4 $\mu$M for F548G, and 26 ± 2 $\mu$M for F548Y protein. TNP-ATP binding could be suppressed by the presence of ADP but not AMP as described previously (*6*, *7*).

*The Dissociation Constant for ATP Was Increased for the R423L, F548G, F548Y, and Q482L Mutants but Not for the I417NN422A and E505Q Mutants of the $H_4-H_5$ Loop.* The dissociation constant of ATP with $Na^+/K^+$-ATPase is ~3 orders of magnitude higher than that of TNP-ATP, as discussed below, suggesting a certain stabilizing role of the trinitrophenyl moiety of the fluorescence probe in the

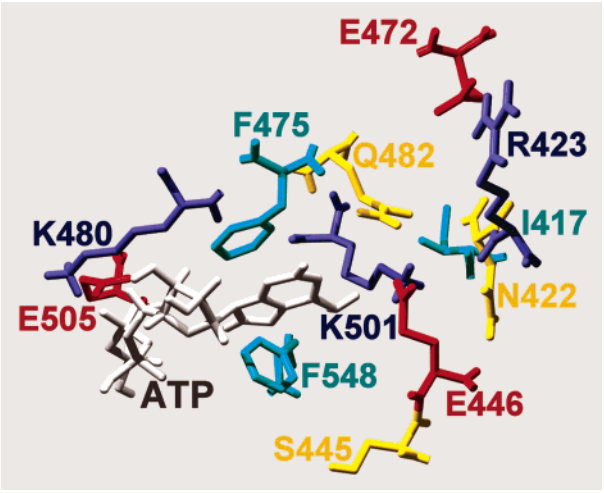


FIGURE 2: Magnification of the ATP-binding site of the N-domain in the presence of ATP. *In silico* docking was performed with the AutoDock program under the conditions described by Ettrich et al. (*5*). $Glu^{446}$, $Phe^{475}$, $Lys^{480}$, $Gln^{482}$, $Lys^{501}$, $Gly^{502}$ (not shown), $Phe^{548}$, and $Cys^{549}$ (not shown) form the ATP-binding pocket. $Ile^{417}$, $Asn^{422}$, and $Ser^{445}$ are too distant to influence the interaction with ATP. The hydrogen bond between $Arg^{423}$ and $Glu^{472}$ is very important for supporting the overall shape of the binding pocket (see Figure 3).

complex with the protein. Hence, one cannot exclude the possibility that the interaction of the trinitrophenyl moiety itself with the protein is affected in our mutants. Therefore, we determined the dissociation constant of ATP−peptide complexes for all constructs as well.

Competition for the binding sites between ATP and TNP-ATP was used to characterize the binding of ATP to the fusion proteins (see Materials and Methods). A lower fluorescence intensity was observed as compared with that from an experiment in the absence of ATP (see Figure 1). This indicated some binding sites are occupied by ATP and allowed us to calculate dissociation constants for ATP. As for TNP-ATP binding, we found that the dissociation constant ($K_D$) for ATP increased from a value of 6.2 ± 0.7 mM for the WT (*9*) protein to 8 ± 2 mM for I417NN422A, 31 ± 9 mM for R423L, 16 ± 4 mM for Q482L, 11 ± 3 mM for F548G, and 24 ± 18 mM for F548Y protein, while the E505Q mutation did not alter the value of the dissociation constant for ATP binding.

## DISCUSSION

The solely expressed $H_4-H_5$ loop−GST fusion protein lacks the interactions with other domains of the sodium pump and is not affected in its structure by $Na^+$- or $K^+$-dependent conformational changes in the transmembrane part. Moreover, it is well-known that this loop has a self-supporting structure (*18*, *34*) and retains the ability to bind ATP (*6*, *7*) and to hydrolyze very slowly *p*-nitrophenyl phosphate in an $Mg^{2+}$-dependent way (*8*). The high-affinity ATP-binding site resides on the N-domain between amino acids I390 and L576 (*13*). This work provides a closer look at the ATP site and reveals the amino acids of the active site in the N-domain with ATP (Figure 2).

The $H_4-H_5$ loop contains N-terminal and C-terminal subdomains of the P-domain and a bulky N-domain. C-Terminal shortening of the $H_4-H_5$ loop−GST fusion proteins down to L576 removes the C-terminal subdomain of the P-domain, and part of the N-domain has been reported to have no effect on the affinity and binding properties of TNP-ATP (*13*). In other words, removal of 200 amino acid residues between L576 and L777 did not significantly change the properties of the ATP-binding site. The model of the $H_4-H_5$ loop (Figure 2) shows that amino acids K480, K501, E505, and F475 are close to the adenosine moiety of TNP-ATP.

A part of the $H_4-H_5$ loop of $Na^+/K^+$-ATPase ($Leu^{354}$–$Ile^{604}$) was used to test the influence of point mutations on the binding of ATP. Infrared spectroscopy revealed no changes in the secondary structure caused by these point mutations, suggesting the observed effects are a consequence of ATP interaction with individual amino acids (*23*). This technique was mainly employed to detect relative changes between the proteins with different point mutations. Notably, the expressed proteins with point mutations are similar in size to the GST protein, which, however, neither interacted with the expressed proteins nor interfered with their structure. Consequently, the sensitivity of FTIR for detection of structural changes of the proteins was satisfactory for our experiments.

The fluorescent analogue of ATP, TNP-ATP, has been used to evaluate these changes in ATP and TNP-ATP dissociation constants. The estimated values of the dissociation constants for the wild-type protein [$K_D$ = 3.1 ± 0.2 $\mu$M for TNP-ATP binding, and $K_D$ = 6.2 ± 0.7 mM for ATP binding (*9*)] were in good agreement with the results from other laboratories for similar constructs (*6*, *8*, *35*).

We have already shown that mutations of $Phe^{475}$ and $Glu^{446}$ resulted in substantial inhibition of TNP-ATP as well as ATP binding to the $H_4-H_5$ loop of $Na^+/K^+$-ATPase (*9*). In fact, our model reveals that the aromatic ring of $Phe^{475}$ and the adenine ring of ATP are parallel at a distance of 0.3 nm. A stacking interaction between their $\pi$-electron systems is important for the stabilization of ATP within the binding pocket. The key role of this residue is also reflected by the substantial inhibition of the activity of the enzyme when it is mutated (*12*). The negatively charged $Glu^{446}$ forms a hydrogen bond over a distance of 0.20 nm to the $NH_2$ hydrogen donor of the adenosine moiety. Because a hydrogen bond can be formed only over a very short distance, the exact position of this residue is crucial for the interaction with ATP. These two residues seem to be the most important ones for the interaction with ATP.

Another residue involved in the ATP-binding pocket could be $Gln^{482}$ as we suggested earlier (*14*). This residue has escaped attention so far, perhaps because it is not conserved in the sequence of $Ca^{2+}$-ATPase. Interestingly, its replacement with leucine has resulted in a strong inhibition of both TNP-ATP and ATP binding. Molecular modeling proposed that the closest distance between this residue and ATP is 0.38 nm and that the mechanism of participation of this residue in ATP recognition is rather indirect. The $NH_2$ group of $Gln^{482}$ stabilizes a side chain of $Glu^{446}$ by a hydrogen bond over a distance of 0.25 nm, attracting the glutamic acid closer to the $NH_2$ group of ATP and thus making it possible for a hydrogen bond to be formed.

Another residue that was examined was $Phe^{548}$ which was replaced with tyrosine and glycine. We have observed a strong inhibition of ATP binding for the F548Y mutant, but only a modest one for the F548G mutant. Notably, the

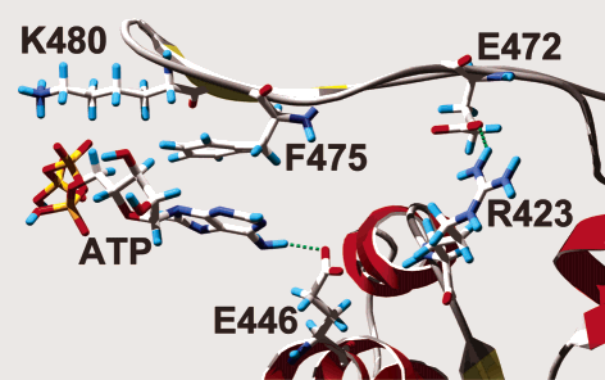


FIGURE 3: Hydrogen bond between $Arg^{423}$ and $Glu^{472}$ that supports the shape of the ATP-binding pocket. The hydrogen bond between $Arg^{423}$ and $Glu^{472}$ over a distance of 0.17 nm brings the stretch of amino acids containing residues $Phe^{475}$, $Lys^{480}$, and possibly also $Glu^{482}$ (not shown) close to other residues involved in ATP binding, such as $Glu^{446}$ and $Lys^{501}$ (not shown).

increase in the TNP-ATP microenvironment polarity within the binding pocket after introduction of the F548Y mutation can, in principle, influence the assessment of the dissociation constant. Fortunately, this effect is likely to be much smaller in magnitude than the observed difference between $K_D$ values for K605 (WT) and F548Y. First, the ATP-binding site is composed of eight amino acids, and thus, one point mutation can hardly cause a dramatic increase in its polarity. Second, we performed model calculations to show that even a relatively large error in the $\gamma$ value estimate would vary the dissociation constant for ATP only moderately; e.g., reducing the $\gamma$ value from 7 to 4 would reduce the calculated $K_D$ (ATP) for F548Y from 24 to 21 mM. We then concluded that, because tyrosine contains a residue more bulky than phenylalanine or glycine, a substantial part of the observed inhibition is due to steric hindrance. A similar conclusion has been drawn for the adjacent residue, $Cys^{549}$. Chemical modification of this residue inhibited ATP binding (*36*), but its replacement with serine or alanine had only a modest influence on the activity of the enzyme (*22*). Therefore, we concluded that although $Phe^{548}$ is only 0.29 nm from the ATP molecule at the smallest separation, this residue plays only a minor role in the direct interaction with ATP. Nevertheless, $Phe^{548}$ belongs to the key amino acid residues supporting and maintaining the structure, as well as the shape of the ATP-binding pocket. Furthermore, the fact that both mutations strongly inhibited TNP-ATP binding indicates that this residue is also involved in the stabilization of the trinitrophenyl moiety. This statement is further supported by a comparison with the structure deduced from X-ray spectroscopy of the crystal of $Ca^{2+}$-ATPase with bound TNP-AMP (*3*).

Surprisingly, the strongest inhibition of ATP binding was observed when the guanidyl residue was missing in the R423L mutant, but the mutation of $Asn^{422}$ and $Ile^{417}$ had only a marginal effect. Abu-Abed et al. (*21*) predicted only a minor role of the corresponding stretch of residues in the $Ca^{2+}$-ATPase in the recognition of ATP. This is in accordance with the predictions from our model where these residues, including $Arg^{423}$, lie outside the ATP-binding pocket. However, $Arg^{423}$ can form a hydrogen bond with $Glu^{472}$ over a distance of 0.17 nm (Figure 3). Breaking this hydrogen bond probably causes an instability in the stretch of amino acids containing residues $Phe^{475}$, $Lys^{480}$, and $Gln^{482}$ within the binding pocket which are in the proximity of the other residues involved in ATP binding, such as $Lys^{501}$ and $Glu^{446}$. This corresponds with the finding that mutations of $Glu^{472}$ lead to a strong inhibition of $Na^+/K^+$-ATPase (*20*). However, this hypothesis must be verified in the future.

We also found that mutations S445A and E505Q had no significant effect on ATP binding. This indicates their minor role in ATP recognition. The fact that these mutations had a modest influence on the binding of the bulkier TNP-ATP indicates their proximity to the binding site.

In conclusion, we showed that besides the previously reported amino acids ($Lys^{480}$, $Lys^{501}$, $Gly^{502}$, and $Cys^{549}$), $Glu^{446}$, $Phe^{475}$, $Gln^{482}$, and $Phe^{548}$ residues also form the ATP-recognizing pocket of $Na^+/K^+$-ATPase. The shape of this pocket is probably stabilized by a hydrogen bond between $Arg^{423}$ and $Glu^{472}$. Mutations of $Ile^{417}$, $Gln^{422}$, $Ser^{445}$, and $Glu^{505}$ did not affect the ATP binding. Molecular modeling of the ATP site within the $H_4-H_5$ loop reveals that the set of these eight amino acids residues forming the ATP recognition site is complete. However, we cannot exclude the possibility that certain amino acid interactions in the structural backbone contribute to the stabilization of the shape of this binding pocket as suggested for $Arg^{423}$ and $Glu^{472}$ (Figure 3). Several other amino acids such as $Asp^{443}$ (*11*), $Arg^{544}$, $Asp^{555}$, $Glu^{556}$, $Asp^{565}$, and $Glu^{567}$ (*22*), $Asp^{710}$ and $Asp^{714}$ (*37*), or $Lys^{766}$ (*38*) were shown to be important for the activity of the whole enzyme. This effect may be explained by an influence on phosphorylation rather than on the binding of ATP itself.

## REFERENCES

1. Kaplan, J. H. (2002) *Annu. Rev. Biochem. 71*, 511−535.
2. Taniguchi, K., Kaya, S., Abe, K., and Mardh, S. (2001) *J. Biochem. 129*, 335−342.
3. Toyoshima, C., Nakasako, M., Nomura, H., and Ogawa, H. (2000) *Nature 405*, 647−655.
4. Toyoshima, C., and Nomura, H. (2002) *Nature 418*, 605−611.
5. Ettrich, R., Melichercik, M., Teisinger, J., Ettrichova, O., Krumscheid, R., Hofbauerova, K., Kvasnicka, P., Schoner, W., and Amler, E. (2001) *J. Mol. Model. 7*, 184−192.
6. Gatto, C., Wang, A. X., and Kaplan, J. H. (1998) *J. Biol. Chem. 273*, 10578−10585.
7. Obsil, T., Mérola, F., Lewit-Bentley, A., and Amler, E. (1998) *FEBS Lett. 426*, 297−300.
8. Tran, C. M., and Farley, R. A. (1999) *Biophys. J. 77*, 258−266.
9. Kubala, M., Hofbauerova, K., Ettrich, R., Kopecky, V., Krumscheid, R., Plásek, J., Teisinger, J., Schoner, W., and Amler, E. (2002) *Biochem. Biophys. Res. Commun. 297*, 154−159.
10. Hebert, H., Purhonen, P., Vorum, H., Thomsen, K., and Maunsbach, A. B. (2001) *J. Mol. Biol. 314*, 479−494.
11. Patchornik, G., Munson, K., Goldshleger, R., Shainskaya, A., Sachs, G., and Karlish, S. J. D. (2002) *Biochemistry 41*, 11740−11749.
12. Teramachi, S., Imagawa, T., Kaya, S., and Taniguchi, K. (2002) *J. Biol. Chem. 277*, 37394−37400.
13. Krumscheid, R., Susankova, K., Ettrich, R., Teisinger, J., Amler, E., and Schoner, W. (2003) *Ann. N.Y. Acad. Sci.* (in press).
14. Hinz, H. R., and Kirley, T. L. (1990) *J. Biol. Chem. 265*, 10260−10265.
15. Tran, C. M., Scheiner-Bobis, G., Schoner, W., and Farley, R. A. (1994) *Biochemistry 33*, 4140−4147.
16. Tran, C. M., Huston, E. E., and Farley, R. A. (1994) *J. Biol. Chem. 269*, 6558−6565.
17. Farley, R. A., Tran, C. M., Carilli, C. T., Hawke, D., and Shively, J. E. (1984) *J. Biol. Chem. 259*, 9532−9535.
18. Abbott, A. J., Amler, E., and Ball, W. J. J. (1991) *Biochemistry 30*, 1692−1701.

19. Gatto, C., Lutsenko, S., and Kaplan, J. H. (1997) *Arch. Biochem. Biophys. 340*, 90−100.
20. Scheiner-Bobis, G., and Schreiber, S. (1999) *Biochemistry 38*, 9198−9208.
21. Abu-Abed, M., Mal, T. K., Kainosho, M., MacLennan, D. H., and Ikura, M. (2002) *Biochemistry 41*, 1156−1164.
22. Jacobsen, M. D., Pedersen, P. A., and Jorgensen, P. L. (2002) *Biochemistry 41*, 1451−1456.
23. Hofbauerova, K., Kopecky, V. J., Ettrich, R., Ettrichova, O., and Amler, E. (2002) *Biopolymers 67*, 242−246.
24. Bradford, M. M. (1976) *Anal. Biochem. 72*, 248−254.
25. Sali, A., and Blundell, T. L. (1993) *J. Mol. Biol. 234*, 779−815.
26. Laskowski, R. A., McArthur, M. W., and Moss, D. S. (1993) *J. Appl. Crystallogr. 26*, 283−291.
27. Morris, G. M., Goodsell, D., Huey, R., and Olson, A. J. (1996) *J. Comput.-Aided Mol. Des. 10*, 293−304.
28. Prokop, M., Damborsky, J., and Koca, J. (2002) *Bioinformatics 16*, 154−159.
29. Baumruk, V., Pancoska, P., and Keiderling, T. A. (1996) *J. Mol. Biol. 259*, 774−791.
30. Hiratsuka, T. (1976) *Biochim. Biophys. Acta 453*, 293−297.
31. Moczydlowski, E. G., and Fortes, P. A. G. (1981) *J. Biol. Chem. 256*, 2346−2356.
32. Kubala, M., Plasek, J., and Amler, E. (2003) *Eur. Biophys. J.* (in press).
33. Kubala, M., Plasek, J., and Amler, E. (2003) *Physiol. Res.* (in press).
34. Amler, E., Abbott, A., and Ball, W. J., Jr. (1992) *Biophys. J. 61*, 553−568.
35. Capiaux, E., Rapin, C., Thines, D., Dypont, Y., and Goffeau, A. (1993) *J. Biol. Chem. 268*, 21895−21900.
36. Linnertz, H., Kost, H., Obsil, T., Kotyk, A., Amler, E., and Schoner, W. (1998) *FEBS Lett. 441*, 103−105.
37. Ovchinnikov, Y. A., Dzhandzhugazyan, K. N., Lutsenko, S. V., Mustayev, A. A., and Modyanov, N. N. (1987) *FEBS Lett. 217*, 111−116.
38. Liu, L., and Askari, A. (1997) *J. Biol. Chem. 272*, 14380−14386.

BI034162U